
Masters Theses

Student Theses and Dissertations

Summer 2020

Experimental evaluation of a honeycomb structure in open channel flows

Kyle David Hix

Follow this and additional works at: https://scholarsmine.mst.edu/masters_theses



Part of the [Hydraulic Engineering Commons](#)

Department:

Recommended Citation

Hix, Kyle David, "Experimental evaluation of a honeycomb structure in open channel flows" (2020).
Masters Theses. 7952.
https://scholarsmine.mst.edu/masters_theses/7952

This thesis is brought to you by Scholars' Mine, a service of the Missouri S&T Library and Learning Resources. This work is protected by U. S. Copyright Law. Unauthorized use including reproduction for redistribution requires the permission of the copyright holder. For more information, please contact scholarsmine@mst.edu.

EXPERIMENTAL EVALUATION OF A HONEYCOMB STRUCTURE IN OPEN
CHANNEL FLOWS

by

KYLE DAVID HIX

A THESIS

Presented to the Graduate Faculty of the
MISSOURI UNIVERSITY OF SCIENCE AND TECHNOLOGY

In Partial Fulfillment of the Requirements for the Degree

MASTER OF SCIENCE IN CIVIL ENGINEERING

2020

Approved by:

Cesar Mendoza, Advisor
Robert Holmes
Katherine Grote

© 2020

Kyle David Hix

All Rights Reserved

ABSTRACT

Designing and controlling open channel flows presents many challenges. One such challenge is energy dissipation. This challenge is currently addressed by several means, including the use of honeycomb structures. Energy dissipation by honeycomb structures has been studied for pressurized conduit flows; however, their ability to dissipate energy in free-surface flows remains largely unexamined. This work introduces a comprehensive experimental study designed to estimate the energy dissipation through a honeycomb structure in a free-surface flow.

This work examined the energy dissipation for a range of flows, pipe lengths, and pipe diameters in two flumes. PVC pipes ranging from 6 inches to 2 feet in length and from $\frac{1}{2}$ inch to 2 inches in diameter were used to build honeycomb structures. These structures were subjected to a range of flows between 0.053 cubic feet per second (cfs) and 4.310 cfs.

A non-linear regression analysis was conducted using SPSS software on the measured data to obtain an empirical dimensionless equation. This empirical equation represents the head losses as a function of discharge and geometric parameters. The parameters in the empirical equation were examined by a sensitivity analysis to determine which parameters are most influential. The results of this work showed that head losses are correlated negatively with the pipe diameter, and positively with the discharge and pipe length.

ACKNOWLEDGMENTS

I would like to thank my Creator for giving me the opportunity and ability to complete this work. I would also like to thank my family and friends for their support and love. I would like to thank my advisor, Dr. Cesar Mendoza for leading me in this pursuit. I would also like to thank my advisory committee, Dr. Robert Holmes and Dr. Katherine Grote, for their support. Finally, I would like to thank my friend Dr. Wesam Mohammed-Ali for his continued encouragement and support.

TABLE OF CONTENTS

	Page
ABSTRACT	iii
ACKNOWLEDGMENTS	iv
LIST OF ILLUSTRATIONS	vii
LIST OF TABLES	ix
SECTION	
1. INTRODUCTION	1
1.1. GENERAL INTRODUCTION	1
1.2. PURPOSE AND SCOPE	1
1.3. THESIS ORGANIZATION	2
2. LITERATURE REVIEW	3
2.1. GENERAL INTRODUCTION	3
2.2. WIND TUNNEL RESEARCH	4
2.3. WATER TUNNEL RESEARCH	5
2.4. OPEN CHANNEL RESEARCH	6
3. THEORY BASE FOR MODEL	8
3.1. SPECIFIC ENERGY	8
3.2. MODELS CONSIDERED	10
3.2.1. Darcy-Weisbach Model	10
3.2.2. FHWA Model	12
3.2.3. Wind Tunnel Model	13
3.3. DIMENSIONAL ANALYSIS	14

4. EXPERIMENTAL WORK	17
4.1. GENERAL INTRODUCTION.....	17
4.2. EXPERIMENTAL WORK DETAILS	17
4.2.1. Experimental Setup.	18
4.2.2. Large Flume.	18
4.2.3. Small Flume.	19
4.2.4. Test Section.	21
4.2.5. Test Model.....	21
4.2.6. FlowTracker.	23
4.2.7. The Measurement Procedures.	24
4.2.8. Summary of Test Conditions.....	25
4.3. STATISTICAL ANALYSIS	29
4.4. EMPIRICAL MODEL DEVELOPMENT	31
4.5. SENSITIVITY ANALYSIS	33
5. RESULTS AND DISCUSSION	39
6. CONCLUSIONS AND RECOMMENDATIONS.....	47
BIBLIOGRAPHY	50
VITA.....	52

LIST OF ILLUSTRATIONS

	Page
Figure 2.1 Types of Honeycombs.....	3
Figure 3.1 Honeycomb Face.....	11
Figure 3.2 Dimensional Analysis Parameters.....	14
Figure 4.1 The 70-Foot Flume Control Panel.....	19
Figure 4.2 Panoramic View of the 70-Foot Flume.....	19
Figure 4.3 The 16-Foot Flume.....	20
Figure 4.4 The 70-Foot Flume Channel.....	22
Figure 4.5 The 16-Foot Flume Channel.....	22
Figure 4.6 Typical Honeycomb Model.....	23
Figure 4.7 FlowTracker2 Probe.....	24
Figure 4.8 SPSS Input Data Windows.....	30
Figure 4.9 Plot of Experimental Values vs Model Values.....	33
Figure 4.10 The Sensitivity Analysis of the Empirical Model to L/D	35
Figure 4.11 The Sensitivity Analysis of the Empirical Model to w/D	36
Figure 4.12 The Sensitivity Analysis of the Empirical Model to y/D	37
Figure 4.13 The Sensitivity Analysis of the Empirical Model to Fr_D	37
Figure 5.1 The Predictability of the Darcy-Weisbach Model.....	40
Figure 5.2 The Predictability of the FHWA Model.....	40
Figure 5.3 The Predictability of the Eckert Model.....	42
Figure 5.4 The Predictability of the Empirical Model.....	42

Figure 5.5 The Plot of h_l/D vs $Q/(g^{1/2}D^{5/2})$ for $w/D = 1$	43
Figure 5.6 The Plot of h_l/D vs $Q/(g^{1/2}D^{5/2})$ for $w/D = 1-1/3$	44
Figure 5.7 The Plot of h_l/D vs $Q/(g^{1/2}D^{5/2})$ for $w/D = 1-1/2$	44
Figure 5.8 The Plot of h_l/D vs $Q/(g^{1/2}D^{5/2})$ for $w/D = 2$	45
Figure 5.9 The Plot of h_l/D vs $Q/(g^{1/2}D^{5/2})$ for $w/D = 2.4$	45
Figure 5.10 The Plot of h_l/D vs $Q/(g^{1/2}D^{5/2})$ for $w/D = 3$	46

LIST OF TABLES

	Page
Table 4.1 Test Conditions for 1 Inch Pipe Honeycombs.	26
Table 4.2 Test Conditions for 1-1/4 Inch Pipe Honeycombs.....	27
Table 4.3 Test Conditions for 2 Inch Pipe Honeycombs.	27
Table 4.4 Test Conditions for 3/4 Inch Pipe Honeycombs.	28
Table 4.5 Test Conditions for 1/2 Inch Pipe Honeycombs.	29
Table 4.6 SPSS Parameter Estimates.....	31
Table 4.7 Empirical Model Performance.....	32
Table 4.8 Model Performance Comparison.	32
Table 4.9 Summary of Sensitivity Analysis.	34
Table 4.10 Sensitivity Analysis Results.....	38
Table 5.1 Model Performance.....	41

1. INTRODUCTION

1.1. GENERAL INTRODUCTION

Many solutions have been suggested and studied for the problem of energy dissipation in open channel flows; one proposed solution is the use of honeycomb structures. The honeycomb structure is an array of stacked up parallel conduits. The energy dissipation phenomenon in a honeycomb has been studied for conduit pressurized flows. However, the energy dissipation in free-surface flows remains largely unexamined.

1.2. PURPOSE AND SCOPE

The purpose of this study is to investigate the head loss through a honeycomb structure in open-channel and provide a design procedure for honeycomb structures for use in an open channel. This was accomplished by reviewing literature related to honeycomb flow conditioner design, determining dimensionless parameters effecting head loss, collecting experimental data and developing an empirical model from a statistical analysis of the experimental data. The empirical model was compared to theoretical models to demonstrate the value of the empirical model. The impact of each parameter was plotted to develop design charts. Additionally, a sensitivity analysis was performed to identify the most influential parameter. The results of the empirical model development and sensitivity analysis were used to develop a design procedure for honeycomb structures.

1.3. THESIS ORGANIZATION

This thesis consists of six Sections. Section 1 contains the general introduction and motivation of this work. Section 2 contains the literature review related to honeycomb flow conditioner design, head loss through honeycombs, and other open channel flow works. Section 3 contains the theory base for the model as well as the theoretical models compared. Section 4 describes the experimental work including design of the experiments, data collection, data analysis, empirical model development, sensitivity analysis and comparison to theoretical models. Section 5 contains the results and discussion of the work. Finally, Section 6 describes the conclusions and recommendations from the study.

2. LITERATURE REVIEW

2.1. GENERAL INTRODUCTION

Flow conditioning is necessary for many applications. Whether it be discharge measurement or component testing, having a predictable flow is critical for confidence in the results. Flow conditioning has been studied in many applications. Much of those studies have been in wind and water tunnel applications and there is some design guidance. However, in open channels, flow conditioning relies on channel length or “rule of thumb” conditioners. This outline defines the terms “flow conditioning” and “honeycomb.” It gives a brief overview of relevant studies in wind and water tunnels as well as research in open channel flows. It also shows the lack of research on honeycomb structures for open channel flow conditioning.

Flow conditioning defines the techniques implemented to produce a known and repeatable velocity profile. Many techniques are currently used. Screens, orifice plates, vanes, approach sections and honeycombs. Prandtl [1] defined honeycombs as “a guiding device through which the individual air filaments are rendered parallel”. This definition applies to water “filaments.” By this definition, honeycombs are flow conditioners. Honeycombs can come in multiple shapes as shown in Figure 2.1 [2].

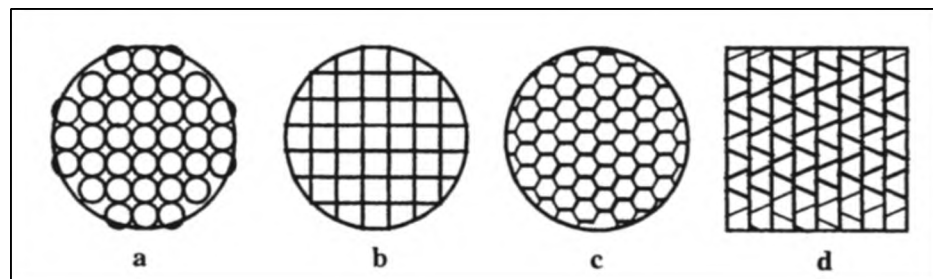


Figure 2.1 Types of Honeycombs [2].

2.2. WIND TUNNEL RESEARCH

Most research on honeycombs has focused on wind tunnel applications. The research ranges from design principles based on experience to turbulence reduction studies. Prandtl [1] described honeycombs and discussed their application principles to wind tunnels. Prandtl recommended depth to division (length to diameter) ratios between 4 and 7 and emphasized the importance of the parallel components in the honeycomb. He further suggested different locations for the honeycomb structure depending on the type of air stream desired and the method employed to produce it. Prandtl's design guidance is based on years of experience in conducting wind tunnel testing. Barlow et al. [2] in more recent design guidance agrees with Prandtl suggesting typical depth to division ratios from 6-8.

Wind tunnel research has evaluated the performance of flow conditioners and provided empirical theories to predict the performance. Scheiman and Brooks [3] noted that empirical theories for performance correlated well with the given experimental data but were unable to consistently predict the performance of a given structure.

The wind tunnel literature on the pressure drop through honeycombs introduced some empirical solutions in terms of the pressure-loss coefficient. The Eckert Equation, as given represented in (1), is one such empirical equations to predict the pressure-loss coefficient. It is reproduced here in the form adopted by Barlow et al. [2]:

$$K_h = \lambda_h \left(\frac{L_h}{D_h} + 3 \right) \left(\frac{1}{\beta_h} \right)^2 + \left(\frac{1}{\beta_h} - 1 \right)^2 \quad (1)$$

where D_h is the hydraulic diameter of the honeycomb cell, β_h is the honeycomb porosity and L_h is the thickness of the honeycomb in the direction of flow,

$$\lambda_h = \begin{cases} 0.375 \left(\frac{\Delta}{D_h} \right)^{0.4} R_{e\Delta}^{-0.1} & \text{for } R_{e\Delta} \leq 275 \\ 0.214 \left(\frac{\Delta}{D_h} \right)^{0.4} & \text{for } R_{e\Delta} > 275 \end{cases} \quad (2)$$

where $R_{e\Delta}$ is the Reynolds number based on material roughness and incoming flow speed, and Δ is the surface roughness in the honeycomb cells. According to Idelcik, Eckert's equation is a simplification of an equation for pressure losses in radiators developed from experimental data [4].

The empirical nature of honeycomb design and implementation and the performance prediction emphasizes the complexity of the problem. Available design guidance relies on rules of thumb and best practices. Additionally, it is abundantly clear from Barlow et al. [2], Scheiman and Brooks [3] and Idelcik [4] that the performance of flow conditioners is difficult to predict and their design follows best practice guidelines .

2.3. WATER TUNNEL RESEARCH

Standard wind tunnel turbulence reduction practice has been translated to water tunnels, but Lumley [5] maintained that those standards can be unacceptable in large water tunnels. Lumley and McMahon [6] reported that the standard wind tunnel practice of using screens was found to be unsuitable due to “singing” effects during vortex shedding in the Garfield Thomas Water Tunnel at the Ordinance Research Laboratory and honeycombs were implemented instead. The effectiveness of honeycombs in water tunnels motivated the studies in Lumley [5] and Lumley and McMahon [6]. These studies centered on the reduction of turbulence intensity immediately downstream of the honeycomb by using Batchelor's approach. This analysis produced design charts for honeycombs in water tunnels if certain parameters are known. These charts provide a

means to design if the turbulence is known. They can be used to estimate the pressure drop coefficient if the ratio of the integral scale of the oncoming turbulence to the cell depth as well as the ratio of final to initial turbulence levels are known. They also can be used to find the pressure drop coefficient if the length to diameter ratio, constant length Reynolds number, and diameter Reynolds are known. The analysis of the collected experimental data provided “good quantitative support” and also showed the efficiency, with respect to the pressure drop, when compared to data for a screen. Lumley found [5] that the honeycomb required $\frac{1}{4}$ the velocity head as that of the screens. Furthermore, these studies introduced a procedure for selecting a turbulence-suppressing honeycomb for application in a water tunnel. The research reported in Lumley [5] and Lumley and McMahon [6] confirmed that honeycombs effectively reduce lateral turbulence but can enhance turbulence as the flow in the components of the honeycomb becomes laminar.

The design process of a water tunnel including a honeycomb was described by Jiang et al. [7]. The honeycomb design was selected based on the nature of the flow in the components of the honeycomb, pressure loss and ease of construction. Although the expected turbulence reduction is thoroughly considered, the pressure drop determination is not mentioned. Water tunnel research begins to bridge the gap between the wind tunnel research and the open channel flow applications.

2.4. OPEN CHANNEL RESEARCH

Flow conditioning in open channels has also received some attention. Most of this research is focused on screens and screen-like structures. Yeh and Shrestha [8] were motivated to study the flow through screens at different inclinations for use in fish

screens. They reported that there was an optimal inclination level to minimize the magnitude of the head loss, but their measurements were slightly different than their model predicted. They noted that transverse bars, an integral structural component of the screen, was likely causing this discrepancy.

The work by Yeh and Shrestha [8] was the basis for the investigation conducted by Çakir [9]. Çakir studied the energy dissipation potential of screens downstream of a sluice gate. The work was limited to the supercritical flow expected to occur downstream of hydraulic structures. In general, it was found that the performance of the screens improved with increases of the Froude number and with a decrease in the ratio of the distance to screen and the height of gate opening. The work added to the range of experimental data on screens in open channels.

Another study on head losses through structures was conducted by Tsikata [10]. He studied the effect of bar and rack geometry on trash racks typically attached to hydropower generating units. The work provides an in-depth analysis of the hydraulic impacts of different trash rack configurations. The work showed that head loss was positively correlated with the approach velocity as well as with the blockage ratio. Additionally, for set bar spacing, the head loss is positively correlated with the bar thickness. Streamlined and rounded bars reduced the head loss. The study provides valuable information for designers and operators generating hydroelectric power plants.

The research work done in open channels covers a limited range of hydraulic structures. Additionally, the work has produced important design guidance for the studied structures. The research, however, has yet to evaluate honeycomb structures.

3. THEORY BASE FOR MODEL

3.1. SPECIFIC ENERGY

The energy equation provides a steady flow equation for frictionless flow. The equation relates pressure, velocity, and elevation. The energy, referred to as head, the sum of the pressure head, the velocity head, and the elevation head. The equation is used to relate the energy of the flow in one location to another. The energy equation is presented in Equation 3

$$\frac{p_1}{\gamma} + \frac{V_1^2}{2g} + z_1 = \frac{p_2}{\gamma} + \frac{V_2^2}{2g} + z_2 + h_f + h_m \quad (3)$$

where p is the pressure, γ is the specific weight, V is the velocity, g is the gravitational acceleration, z is the depth, h_f is the friction head loss, and h_m is the minor head loss.

On the downstream side of the equation the head loss terms are included. The head loss in open channels can be simplified to two terms, friction loss and minor loss. Friction losses are a result of the interaction of the fluid with the channel boundary. The minor losses are a result of changes in the movement of the fluid, typically caused by changes to channel geometry or obstructions in the channel. Many ways to predict the friction loss have been developed and well tested. However, minor losses rely strongly on experimental work.

Minor losses are typically given as a ratio of the head loss to the velocity head and are determined using a loss coefficient [11]. The equation showing the relation of minor losses to velocity head and the loss coefficient (K) as presented by White is reproduced in Equation 4

$$K = \frac{h_m}{v^2/2g} = \frac{\Delta p}{\frac{1}{2}\rho v^2} \quad (4)$$

where ρ is the density.

The energy equation can be simplified for open channel flows in the form of specific energy [11]. The specific energy consists of the flow depth and the velocity head and represents the height of the Energy Grade Line. The specific energy equation is presented in Equation 5.

$$E = y + \frac{v^2}{2g} \quad (5)$$

where y is the depth of flow and E is the specific energy.

The specific energy can be used to compare different energy values for the same discharge rate. For this work the specific energy principle is used to measure the head loss through the test section. The measured head loss is determined using Equation 6

$$y_1 + \frac{v_1^2}{2g} = y_2 + \frac{v_2^2}{2g} + h_l \quad (6)$$

where h_l is the head loss.

This is done because the flumes are leveled, elevation upstream is equal to elevation downstream. Additionally, friction losses from the channel can be neglected since the measurements occur immediately upstream and downstream of the structure. Since the velocity was not measured directly, rather the discharge was measured, Equation 4 must be adjusted. The continuity equation relates the discharge, velocity and area of flow. The continuity equation is presented in Equation 7

$$Q = V * A \quad (7)$$

where Q is the volumetric discharge and A is the flow area.

Combining Equations 6 and 7 results in the final form of the specific energy equation for this work. This form was used to determine the head loss through the honeycomb using the experimental measurements and is presented as Equation 8

$$y_1 + \frac{Q_1^2}{2g(w_c y_1)^2} = y_2 + \frac{Q_2^2}{2g(w_c y_2)^2} + h_l \quad (8)$$

where w_c is the width of the channel.

3.2. MODELS CONSIDERED

Three theoretical models were proposed to predict the head loss through the honeycomb structure. The first, the Darcy-Weisbach model, predicts flow through a pipe. The second, the FHWA culvert equation model, considers flow through a conduit that is either full or partially full. The final, the Eckert Equation model, predicts the head loss coefficient for honeycomb structures in wind tunnels. Each model was developed for different uses but are applied here to examine their usefulness and to support the need for developing an empirical model.

3.2.1. Darcy-Weisbach Model. The Darcy-Weisbach equation predicts the friction head loss through a pipe by considering its length, its diameter, the dimensionless friction factor, and the velocity head as seen in the form

$$h_f = f \frac{L}{d} \frac{V^2}{2g} \quad (9)$$

where f is the friction factor, L is the length of pipe, and d is the pipe diameter.

Equation 9 was applied to each pipe in the structure. The friction factor was estimated from the Moody diagram based on the material characteristics and the

assumption of fully turbulent flow. As shown in Figure 3.1, due to the geometry of the honeycomb structure, non-circular conduits exist.

White [11] provides a means of predicting the friction head loss by replacing the diameter with the hydraulic diameter. The hydraulic diameter, D_h , is estimated as

$$D_h = \frac{4 \cdot A}{P} \quad (10)$$

where A is the cross-sectional area and P is the wetted perimeter.



Figure 3.1 Honeycomb Face.

The minor loss equation, Equation (4), was used to model the entrance and exit losses for each conduit. Standard loss coefficients of 0.5 and 1 were used for the entrance and exit, respectively. In order to apply the model to the experimental observations, some simplifying assumptions were introduced. It was assumed that the average velocity of the flow upstream of the structure is uniformly distributed across the face of the structure. The irregular pipe sections along the boundary of the channel and the structure were not modeled as it was assumed that losses through these channels comprised a negligible portion of the total loss. The model was implemented by determining the head loss for

one representative pipe, both regular and irregular then multiplying that loss by the total number of each pipe in the flow area. The head loss determined included the Darcy-Weisbach friction head losses and the minor losses.

3.2.2. FHWA Model. The second model applied the FHWA culvert equations for head loss. The outlet controlled full-flow head loss equation was applied to all pipes but those in the top layer of pipes in the flow area. The full flow head loss equation is calculated as

$$H = \left[1 + k_e + \frac{K_u n^2 L}{R^{1.33}} \right] \frac{V^2}{2g} \quad (11)$$

where H is the barrel loss, k_e is the entrance loss coefficient, K_u is a unit constant (29 in English units), n is Manning's roughness coefficient, and R is the hydraulic radius.

The outlet control partial flow head loss equation was applied to the top row of pipes in the flow area. First, the criteria for partial flow, $TW > D$ (TW is the tailwater depth and D is the pipe diameter), was confirmed by comparing the tailwater depth to the diameter of the pipe. T

When using Equation (10), the tailwater depth was taken as the depth of flow from the bottom of the pipe to the free surface on the downstream end of the pipe. Once partial flow was confirmed, the critical depth for the pipe was determined. Following the Texas DOT manual [12], the following three equations were solved iteratively to find the critical depth.

$$Q^2/g = A_c^3/T_c \quad (12)$$

where A_c is the area at critical depth and T_c is the top-width at critical depth,

$$A_c = \frac{D^2}{8} \left[2 \cos^{-1} \left(1 - \frac{2d_c}{D} \right) - \sin \left(2 \cos^{-1} \left(1 - \frac{2d_c}{D} \right) \right) \right] \quad (13)$$

where d_c is the critical depth,

$$T_c = D \sin \left(\cos^{-1} \left(\frac{2d_c - D}{D} \right) \right) \quad (14)$$

Once the critical depth was determined for a given iteration, the head loss was computed using the empirical formula given by Mays [13].

$$H = HW_o - h_o \quad (15)$$

where HW_o is the headwater depth above the outlet invert and h_o is determined from [13].

$$h_o = \max \left[TW, (D + d_c)/2 \right] \quad (16)$$

The full flow head loss and partial flow head loss were combined to determine the total predicted head loss.

3.2.3. Wind Tunnel Model. The third model used the Eckert equation originally developed from experimental data. This equation comes from wind tunnel research data and predicts the loss coefficient for use in the minor loss equation, Equation (4).

$$K_h = \lambda_h \left(\frac{L_h}{D_h} + 3 \right) \left(\frac{1}{\beta_h} \right)^2 + \left(\frac{1}{\beta_h} - 1 \right)^2 \quad (17)$$

where D_h is the hydraulic diameter of the honeycomb cell, β_h is the honeycomb porosity and L_h is the thickness of the honeycomb in the direction of flow,

$$\lambda_h = \begin{cases} 0.375 \left(\frac{\Delta}{D_h} \right)^{0.4} R_{e\Delta}^{-0.1} & \text{for } R_{e\Delta} \leq 275 \\ 0.214 \left(\frac{\Delta}{D_h} \right)^{0.4} & \text{for } R_{e\Delta} > 275 \end{cases} \quad (18)$$

where $R_{e\Delta}$ is the Reynolds number based on material roughness and incoming flow speed, and Δ is the surface roughness in the honeycomb cells.

The parameters for the equation were determined for each test model and flow regime. The predicted loss coefficient was used in combination with Equation (2) to determine the predicted head loss.

3.3. DIMENSIONAL ANALYSIS

It is well established that dimensional analysis is an effective tool for simplifying complex phenomenon and directing experimental data collection programs. Additionally, dimensional analysis can simplify the experimental results to the point that they are easily accessible [11, 14]. A dimensional analysis was conducted to determine the effects of the intervening parameters on the minor loss through the honeycomb structure. The results of the dimensional analysis informed the experimental setup and the development of the empirical model. Dimensional analysis was conducted on the squarely packed honeycomb structure shown in Figure 3.2.

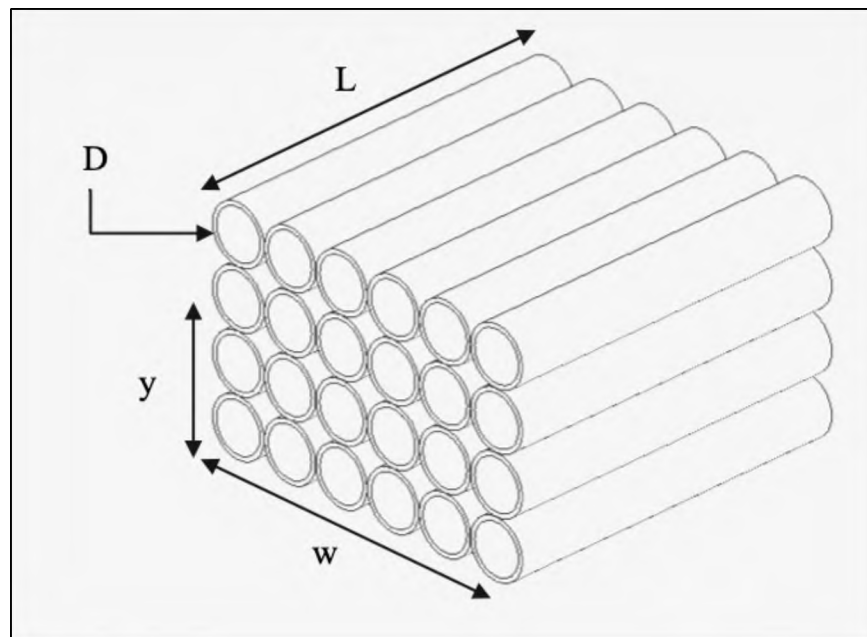


Figure 3.2 Dimensional Analysis Parameters.

The variables pertinent to head loss through the honeycomb were identified. The geometric variables were the diameter of the pipes, D , the depth of the pipes, L , and the width of the structure, w . The flow property variables were the discharge, Q , and the height of the free surface, y . The fluid property variables were the mass density, ρ , the dynamic viscosity, μ , and the acceleration due to gravity, g .

The formula for head loss, h_l , through the structure can be written as a function of the intervening variables as

$$h_l = f(D, L, w, y, Q, g, \rho, \mu) \quad (20)$$

Then, the number of variables N is equal to 9

$$\phi_1(h_l, D, L, w, y, Q, g, \rho, \mu) = 0 \quad (21)$$

The above parameters in dimensional form are, $L, L, L, L, L, \frac{L^3}{T}, \frac{L}{T^2}, \frac{M}{L^3}, \frac{M}{LT}$,

therefore, the number of dimensions is three and the number of π groups is determined,

$9-3 = 6$. The primary variables are (ρ, g, D) . Equation (21) is now written as,

$$\phi_2(\pi_1, \pi_2, \pi_3, \pi_4, \pi_5, \pi_6) = 0 \quad (22)$$

$$\phi_3\left(\frac{Q}{g^{\frac{1}{2}}D^{\frac{5}{2}}}, \frac{\mu}{\rho g^{\frac{1}{2}}D^{\frac{3}{2}}}, \frac{L}{D}, \frac{w}{D}, \frac{y}{D}, \frac{h_l}{D}\right) = 0 \quad (23)$$

The term $\left(\frac{Q}{g^{\frac{1}{2}}D^{\frac{5}{2}}}\right)$ represents Froude's Number, and will be called the Diameter

Froude Number (Fr_D), and the term $\left(\frac{\mu}{\rho g^{\frac{1}{2}}D^{\frac{3}{2}}}\right)$ represents Reynolds Number (Re). Equation

(23) can be rewritten as

$$\phi_4\left(Fr_D, Re, \frac{L}{D}, \frac{w}{D}, \frac{y}{D}, \frac{h_l}{D}\right) = 0 \quad (24)$$

Finally,

$$\frac{h_l}{D} = \phi_5 \left(Fr_D, Re, \frac{L}{D}, \frac{w}{D}, \frac{y}{D} \right) \quad (25)$$

For this work, values for Re ranged from 4473 to 35784 which can be considered fully turbulent [13]. Since the flow is turbulent, the Reynolds number parameter was dropped from Equation (25) and the simplified functional equation became

$$\frac{h_l}{D} = \phi_5 \left(Fr_D, \frac{L}{D}, \frac{w}{D}, \frac{y}{D} \right) \quad (26)$$

Equation (26) is the foundation of the empirical model.

4. EXPERIMENTAL WORK

4.1. GENERAL INTRODUCTION

In this section, the experimental facilities, equipment, measuring techniques, conditions and procedures are described. The experimental results and analysis of the data is also presented. Finally, the development of the empirical model is introduced.

The experiments were conducted on two scales with a range of pipe diameters and lengths. The ranges of the experimental work were selected to evaluate the parameters identified in the dimensional analysis. Details about the experimental work including setup, facilities, equipment, and models are described in Section 4.2. The experimental setup is described in Section 4.2.1. Sections 4.2.2 and 4.2.3 describe the two flumes used in the tests. The test section and test models are described in Sections 4.2.4 and 4.2.5. Section 4.2.6 and 4.2.7 describe the measurement equipment and procedure respectively. Finally, Section 4.2.8 summarizes the test conditions for each series of parameters.

The results of the experimental work were subjected to statistical analysis. The statistical analysis is described in Section 4.3. The outcome of the statistical analysis was the empirical model developed for the conditions of the experiment. The model is discussed in Section 4.4.

4.2. EXPERIMENTAL WORK DETAILS

The experimental work details are included in sections 4.2.1 to 4.2.9. Each section describes one aspect of the experimental work.

4.2.1. Experimental Setup. The experiments were conducted in two flumes at the Missouri University of Science and Technology Hydraulics Lab. The tests were separated into series depending on the pipe diameter and were conducted for a range of dimensionless parameters. The w/D values ranged from 1 to 3, the L/D values ranged 0.5 to 2.67, the y/D values ranged from 1 to 5. Finally, the pipes were tested at a range of discharges from 0.053 to 4.310 cubic feet per second (cfs). Tests on honeycomb structures built with 1", 1.25" and 2" diameter pipes were conducted in the 70-foot flume. Tests on honeycomb structures built with 1", $\frac{3}{4}$ " and $\frac{1}{2}$ " in diameter pipes were conducted in the 16-foot flume. Discharges were measured directly with a SonTek Flowtracker in the 70-foot flume and with built in orifice meters in the 16-foot flume. The depth of flow was measured upstream and downstream of the honeycomb structure. The results of the experimental observations were used to develop the empirical equation.

4.2.2. Large Flume. The large flume in the hydraulics lab was used for large diameter pipes. The flume is 70 feet long, 3 feet deep and 3 feet wide. The channel is constructed of clear acrylic sides and had a cement false bottom. The flume is supported by a steel frame. The flume slope can be changed by varying the elevation of the flume upstream end. For these experiments conducted for this work, the flume was maintained at a horizontal grade. The flume was serviced by 4 pumps; two large and two small. The large pumps are driven by MagnaTek D-390821-02 100 hp motors. The small pumps are driven by MagnaTek 7-860099-01-OJ 16 hp motor. The large pumps are Bell & Gossett 6G 12.250 BF pumps. They can produce 1250 gallons per minute (gpm) and 150 ft of head. The small pumps are Bell & Gossett 3B 9.125 BF pumps. They can produce 400 gpm and 75 ft of head. The pumps are controlled using InTouch WindowViewer software. The

control panel allows the user to select pumps to use and then determine the pump speed of the pumps. The control panel is presented in Figure 4.1. In this work, the two large pumps were both used. A panoramic view of the 70-ft long flume is shown in Figure 4.2.

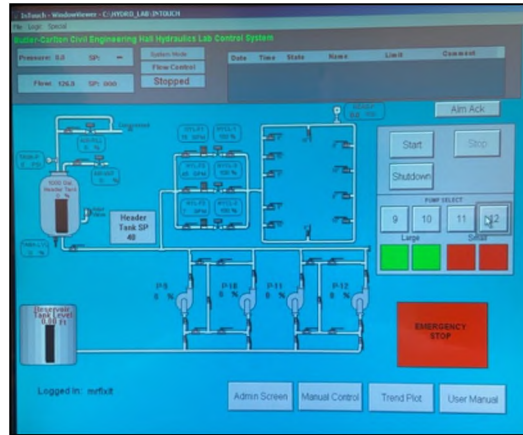


Figure 4.1 The 70-Foot Flume Control Panel.



Figure 4.2 Panoramic View of the 70-Foot Flume.

4.2.3. Small Flume. The small flume in the hydraulics lab was used for testing honeycomb structures made with small diameter pipes.

The flume is a model B-16 Hydraulic Demonstration Channel, designed and built by Engineering Laboratory Design Inc. The flume channel is 16 feet long, 1 foot wide, and 1.5 feet deep. The channel is constructed of 0.5 in thick clear acrylic. Figure 4.3 shows the 16 ft flume.



Figure 4.3 The 16-Foot Flume.

The flume reservoir, which holds approximately 136 gallons of water, serves the two flume pumps. The pumps are low head, high volume pumps (Price Pump Model XT200AB-525-21111-75-18C-1D6) and are powered by Baldor Model No. 34F181W198 motors. Each pump delivers 95 gallons per minute (gpm) at 25 feet of head for a maximum total flow of 190 gpm. Two orifice flow meters are available for flow discharge measurements. The orifice flow meters are read using a U-tube manometer and a calibration curve. The calibration equation for the small orifice flow meter in (ft^3/s) is

$$Q = 0.0554 * \sqrt{\Delta h_{(\text{ft})}} \quad (27)$$

where Δh is the manometric reading height in feet. The calibration equation for the large orifice flow meter in (ft^3/s) is

$$Q = 0.2009 * \sqrt{\Delta h_{(\text{ft})}} \quad (28)$$

The calibration equations were used to determine the discharge during the small-flume experiments. The flume utilizes a headtank to reduce turbulence from the pumps.

The headtank has a headgate to control the pressure of the flow in the flume. The headgate was raised so it had no effect on the experiments. The flume also has a tailgate for flow depth control. The flume was leveled, and the tailgate lowered parallel to the channel bed for the testing.

4.2.4. Test Section. The test section was located near the middle of each flume. This provided significant distance downstream from the stilling basin for the flow to be uniform and fully developed. The test section materials were consistent with the rest of the flume channel. In the 70-Foot flume the side walls were clear acrylic and the bed cement. In 16-Foot flume all bounding sides were clear acrylic. The cross-sectional area of the test section was rectangular uniform with the rest of the channel geometry as well. For models that didn't fit flush with the side walls spacers were used to close the gap on one side. The spacers forced the flow to go through the structure so head loss could be attributed to the structure itself. The models were assembled in the test section and altered as needed. The models were aligned parallel to the direction of flow within the test section. Models were secured by setting small steel beams or plates on top of the structure. Typical channel sections, representative of the test sections, are shown in Figures 4.4 and 4.5.

4.2.5. Test Model. The test models consisted of readily available PVC pipes cut to length and assembled as a squarely stacked honeycomb. Five pipe diameters were tested: $\frac{1}{2}$ ", $\frac{3}{4}$ ", 1", 1-1/4" and 2" (NPS) notation. The pipes were cut to 2 feet in length, 1 foot in length and 0.5 feet in length. These lengths provided L/D ratios of 0.5 to 2.67.

The pipes were stacked vertically on center. For each honeycomb structure, the pipes were secured using static friction aided with weight distributed along the top of the

structure. The weight was in the form of two, 3-foot long steel I-beams or four steel plates stored in the lab. The honeycomb was oriented so that the pipes were parallel to the channel. A typical non-staggered honeycomb assembly can be seen in Figure 4.6.



Figure 4.4 The 70-Foot Flume Channel.



Figure 4.5 The 16-Foot Flume Channel

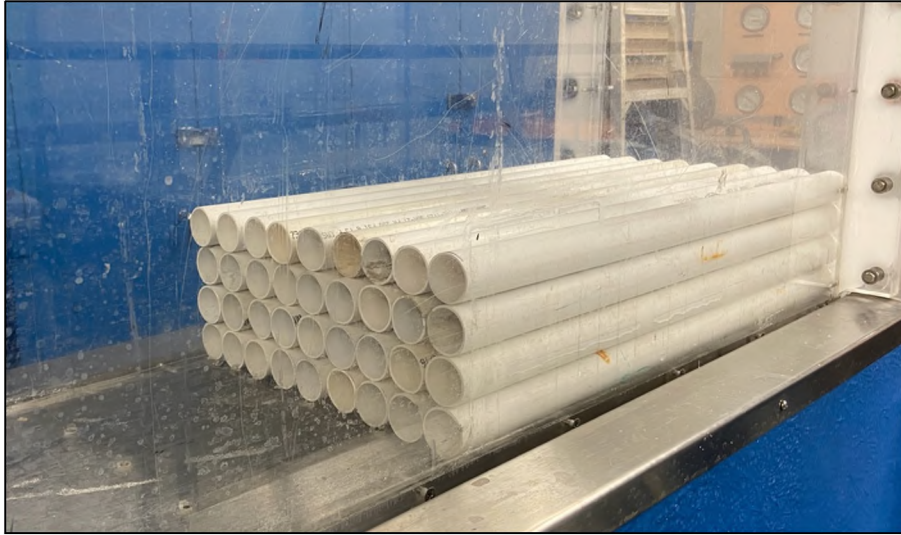


Figure 4.6 Typical Honeycomb Model.

4.2.6. FlowTracker. The SonTek FlowTracker is an acoustic doppler velocimeter (ADV). It utilizes Doppler shift to measure the velocity of the flow. The Doppler principle states that the frequency of the sound transmitted to a receiver shifts if the source of the sound is moving relative to the receiver.

$$F_{\text{doppler}} = F_{\text{source}} * \left(\frac{V}{C} \right) \quad (29)$$

where, F_{doppler} is the Doppler shift, F_{source} is the transmitted frequency, V is the velocity of the source relative to the receiver, and C is the speed of sound. The FlowTracker is a bi-static Doppler current meter which means the transmitter and receiver are located on the same probe. The receivers are mounted such that sampling beams intersect in a volume of water 4 in from the tip of the probe. The transmitted acoustic beam is reflected by particles in the water and the modified frequency is sampled by the receivers. The Doppler shift is used to determine the velocity using Equation (29). The probe alignment can be seen in Figure 4.7.

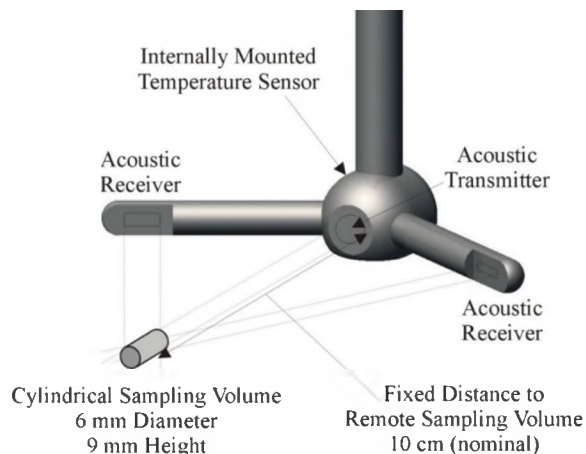


Figure 4.7 FlowTracker2 Probe.

The FlowTracker can measure velocities in the range between 0.003 and 13 feet per second (ft/s) with accuracies up to 1% of measured velocity for each one-second sample. These characteristics made this instrument well suited for the large-flume experiments where the expected velocities were less than 4 ft/s. It is assumed that the velocity of the particles represents the velocity of the water itself. The FlowTracker automatically calculates the discharge using the Mid-Section, Mean-Section, or the Japanese Equation method. For the large scale experiments the Mid-section method was selected. The mean velocity was sampled at 0.6 of the flow depth. Since the channel was uniform and rectangular, only one measurement was made at mid-channel.

4.2.7. The Measurement Procedures. Although the measurement procedures for the large-scale and the small-scale tests were similar, some differences worth reporting were also implemented. In the large-scale tests the discharge was adjusted using the flume control software to change the pump speed. Discharge was set such that the flow depth at the upstream end of the structure was flush with the top of a given row in the structure. The flow was given ample time to stabilize at each depth. The SonTek

FlowTracker2 was used to obtain the discharge. The measurement was taken in the middle of the channel at a location approximately 12-12.5 feet upstream of the structure. Once the discharge was measured, the upstream and downstream depth were measured on each side of the flume. Five sets of depth measurements were taken. The depth was recorded using a scale fixed to the exterior face of the flume. The depth was measured from the bed to the free surface. The downstream flow depth was measured at the vena contracta in the downstream discharge using a non-fixed scale. The averaged depths were used in the calculation of head loss. After the depths were measured the discharge was adjusted and the process repeated.

In the small-scale experiments the discharge was adjusted using the gate valves near the upstream end of the flume. The discharge was set such that the flow depth at the upstream end of the structure was flush with the top of a given row in the honeycomb structure. The flow was given ample time to stabilize at each depth. The orifice meters were read and recorded. Once the discharge was measured, the upstream and downstream depth was measured on either side of the flume. Five sets of depth measurements were taken. The depth was recorded using a Vernier Scale. The depth to the bed was measured and then the depth to the free surface. The difference in the two measurements represented the flow depth. The downstream depth was measured at the vena contracta in the downstream discharge following the same method as upstream. After the depths were measured the discharge was adjusted and the process repeated.

4.2.8. Summary of Test Conditions. The test conditions for each series of tests are summarized in Tables 4.1- 4.5. The water properties and environmental conditions were kept constant throughout the experimental work. The series were separated by pipe

diameter and summarized below. The width and length units for the parameters were in feet while the flow depth and diameter units were in inches. The discharge units were cubic feet per second.

The 1 Inch pipe was tested in 12 separate scenarios. The pipes were tested in both the small flume and the large flume resulting in w/D values of 2 and 3. The pipes were also tested at two lengths resulting in L/D values of 1 and 2. The pipes were tested at multiple y/D values, depending on the test flume used, resulting in a range from 1 to 5. Finally, the pipes were tested at a range of discharges from 0.093 to 2.662 cubic feet per second (cfs). The summary of the 1 Inch Pipe tests is given in Table 4.1.

Table 4.1 Test Conditions for 1 Inch Pipe Honeycombs.

Test	Q (cfs)	L/D	w/D	y/D	h_L
D=1 (1)	0.093	1	1	1	0.014
D=1 (2)	0.251	1	1	2	0.037
D=1 (3)	0.428	1	1	3	0.047
D=1 (4)	0.064	2	1	1	0.018
D=1 (5)	0.226	2	1	2	0.042
D=1 (6)	0.415	2	1	3	0.069
D=1 (7)	1.099	1	3	3	0.068
D=1 (8)	1.927	1	3	4	0.093
D=1 (9)	2.662	1	3	5	0.106
D=1 (10)	1.077	2	3	3	0.084
D=1 (11)	2.003	2	3	4	0.111
D=1 (12)	2.662	2	3	5	0.123

The 1-1/4 Inch pipe was tested in 6 separate scenarios. The pipes were tested in the large flume resulting in a w/D value of 2.4. The pipes were tested at two lengths resulting in L/D values of 1.6 and 0.8. The pipes were tested at y/D values in the range between 2 and 4. Finally, the pipes were tested at a range of discharges from 1.227 to 3.914 cfs. The summary of the 1-1/4 Inch Pipe tests is given in Table 4.2.

Table 4.2 Test Conditions for 1-1/4 Inch Pipe Honeycombs.

Test	Q (cfs)	L/D	w/D	y/D	h_L
D=1.25 (1)	1.227	1.6	2.4	2	0.055
D=1.25 (2)	2.330	1.6	2.4	3	0.072
D=1.25 (3)	3.177	1.6	2.4	4	0.075
D=1.25 (4)	1.246	0.8	2.4	2	0.060
D=1.25 (5)	2.396	0.8	2.4	3	0.101
D=1.25 (6)	3.914	0.8	2.4	4	0.101

The 2 Inch pipe was tested in 6 separate scenarios. The pipes were tested in the large flume resulting in a w/D value of 1.5. The pipes were tested at two lengths resulting in L/D values of 1 and 0.5. The pipes were tested for y/D values in the range from 1 to 3. Finally, the pipes were tested in the range of discharges from 0.572 to a 4.31 cfs. The summary of the 2 Inch Pipe tests is presented in Table 4.3.

Table 4.3 Test Conditions for 2 Inch Pipe Honeycombs.

Test	Q (cfs)	L/D	w/D	y/D	h_L
D=2 (1)	0.573	1	1.5	1	0.044
D=2 (2)	1.213	1	1.5	2	0.111
D=2 (3)	3.720	1	1.5	3	0.115
D=2 (4)	0.572	0.5	1.5	1	0.045
D=2 (5)	2.322	0.5	1.5	2	0.057
D=2 (6)	4.310	0.5	1.5	3	0.079

Nine separate test were conducted with the 3/4-inch pipe. These pipes were tested in the small flume resulting in a w/D value of 1.33. The pipes were tested at three lengths resulting in L/D values of 2.67, 1.33, and 0.67. The pipes were tested in a range of y/D from 2 to 4. Finally, the pipes were tested in a range of discharges between 0.120 and 0.379 cfs. The summary of the 3/4 Inch Pipe tests is presented in Table 4.4.

Table 4.4 Test Conditions for 3/4 Inch Pipe Honeycombs.

Test	Q (cfs)	L/D	w/D	y/D	h_L
D=3/4 (1)	0.334	2.67	1.33	4	0.119
D=3/4 (2)	0.224	2.67	1.33	3	0.084
D=3/4 (3)	0.125	2.67	1.33	2	0.047
D=3/4 (4)	0.379	1.33	1.33	4	0.093
D=3/4 (5)	0.252	1.33	1.33	3	0.071
D=3/4 (6)	0.120	1.33	1.33	2	0.043
D=3/4 (7)	0.365	0.67	1.33	4	0.078
D=3/4 (8)	0.260	0.67	1.33	3	0.064
D=3/4 (9)	0.136	0.67	1.33	2	0.040

The 1/2 Inch pipe was tested in 9 separate scenarios. The pipes were tested in the small flume; the w/D ratio has a value of 2. The pipes were tested at three lengths resulting in L/D values of 4, 2, and 1. The pipes were tested at y/D values in the range from 2 to 4. Finally, the pipes were tested in a range of discharges from 0.053 to 0.284 cfs. The summary of the 1/2 Inch Pipe tests is presented in Table 4.5.

Table 4.5 Test Conditions for 1/2 Inch Pipe Honeycombs.

Test	Q (cfs)	L/D	w/D	y/D	h _L
D=1/2 (1)	0.226	4	2	4	0.114
D=1/2 (2)	0.130	4	2	3	0.076
D=1/2 (3)	0.053	4	2	2	0.042
D=1/2 (4)	0.254	2	2	4	0.084
D=1/2 (5)	0.157	2	2	3	0.061
D=1/2 (6)	0.073	2	2	2	0.032
D=1/2 (7)	0.284	1	2	4	0.069
D=1/2 (8)	0.180	1	2	3	0.056
D=1/2 (9)	0.076	1	2	2	0.027

4.3. STATISTICAL ANALYSIS

A non-linear regression of the experimental data collected was conducted using the IBM software SPSS Statistics to determine an empirical model equation in line with the functional equation derived by dimensional analysis. The general form of the empirical model is

$$\frac{h_L}{D} = x_1 \left(\frac{L}{D}\right)^{x_2} * x_3 \left(\frac{w}{D}\right)^{x_4} * x_5 \left(\frac{y}{D}\right)^{x_6} * x_7 (Fr_D)^{x_8} \quad (30)$$

where the coefficients x_1 through x_8 are constants to be determined from the non-linear regression, $\frac{h_L}{D}$ is the ratio of the head loss in feet to the pipe diameter in inches, Fr_D is the Diameter Froude Number, $\frac{L}{D}$ is the ratio of the depth of pipe in feet to the pipe diameter in inches, $\frac{w}{D}$ is the ratio of the structure width in feet to the pipe diameter in

inches, and $\frac{y}{D}$ is the ratio of the free-surface height in inches to the pipe diameter in inches. The experimental observations were randomized and split into two groups. The data were assigned random numbers and then ordered from smallest to largest. The first group was used in the regression analysis to determine the coefficients and represented the first 3/4th of the randomized data. The second group was used for validation of the model and represented the remaining 1/4th of the randomized data. Figure 4.8 shows the SPSS input and Table 4.6 summarizes the values of the calculated parameters.

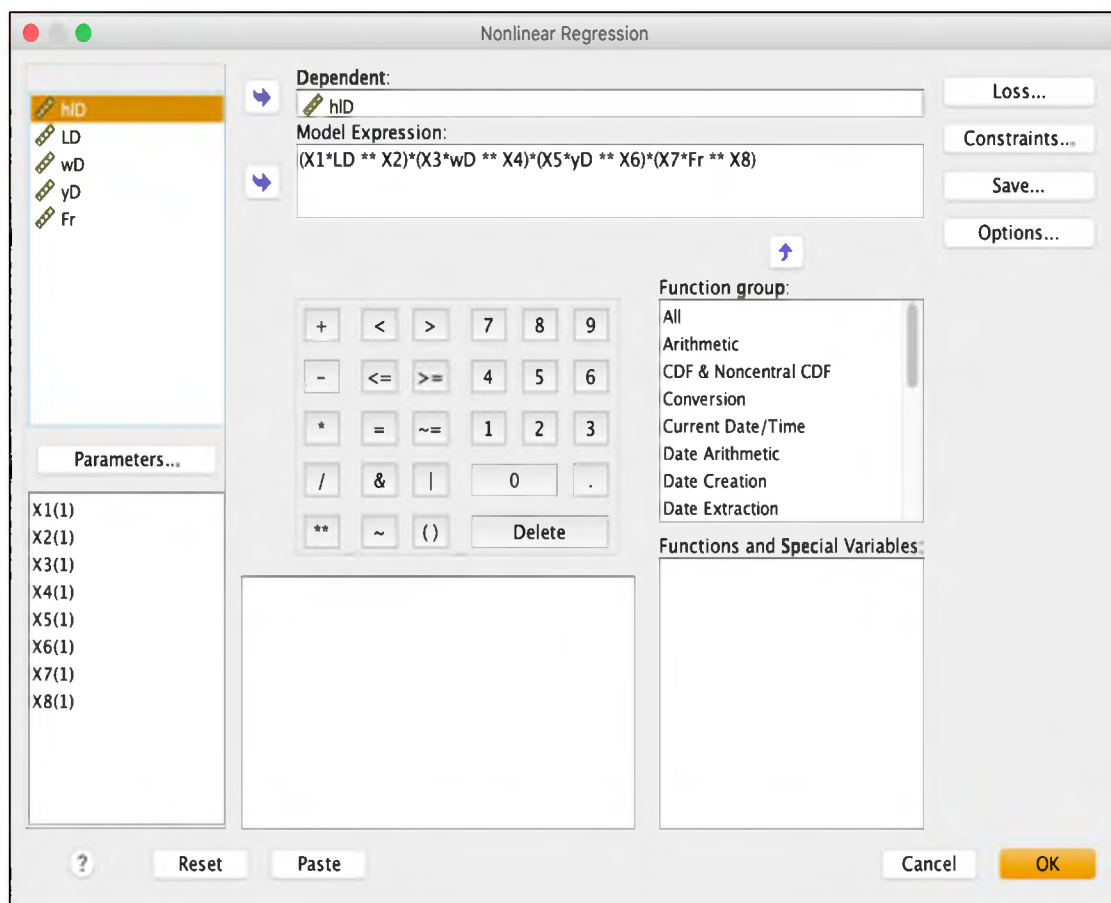


Figure 4.8 SPSS Input Data Windows.

Table 4.6 SPSS Parameter Estimates.

Parameter	Estimate
X1	0.70
X2	0.49
X3	0.53
X4	-0.23
X5	0.32
X6	1.04
X7	0.24
X8	0.06

4.4. EMPIRICAL MODEL DEVELOPMENT

The empirical model equation was developed from the statistical analysis. Thus, Equation (4) is now written as

$$\frac{h_l}{D} = 0.029 \left(\frac{L}{D}\right)^{0.49} \left(\frac{w}{D}\right)^{-0.23} \left(\frac{y}{D}\right)^{1.04} Fr_D^{0.06} \quad (31)$$

The performance of the empirical model was evaluated using the Nash-Sutcliffe model efficiency coefficient, NSE [15]

$$NSE = 1 - \frac{\sum_t (O - S)^2}{\sum_t (O - \bar{O})^2} \quad (32)$$

where O is the observed variable, S is the simulated variable and \bar{O} is the average of the observed variable.

The NSE was chosen because it evaluates how well a model predicts observed values in a established timescale. The timescale is the series of measurements for the empirical model. The NSE is often used to gauge the efficiency of hydrologic models, e.g. Mohammed-Ali et al. [16, 17]. An NSE value of 1 represents a model that perfectly predicts the observed condition. A value of zero means the model will predict the mean value of the observed events. Negative values represent models that don't predict better than the mean value. The numerical value of the parameters was obtained from the statistical analysis and then the NSE was computed for the validation portion of the data. Additionally, the NSE was computed for the model development portion of the data. The model performance parameters are summarized in Table 4.7.

Table 4.7 Empirical Model Performance.

Parameters	Development	Validation
NSE	0.83	0.75

The model performance parameters for the considered models is summarized in Table 4.8.

Table 4.8 Model Performance Comparison.

Model	NSE
Empirical	0.75
Darcy	-72939
FHWA	-53526
Eckert	-16.2

Figure 4.9 shows the plot of the experimental dimensionless head loss to modeled head loss. The performance of the empirical derived model was compared with the results of the other models considered. The empirical model performed the best out of the models considered.

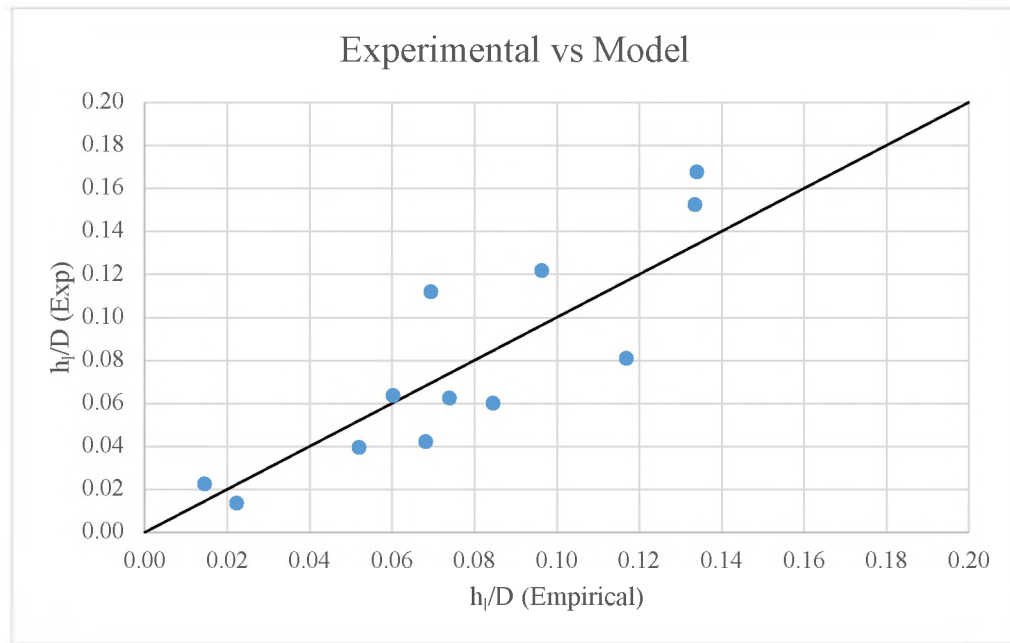


Figure 4.9 Plot of Experimental Values vs Model Values.

4.5. SENSITIVITY ANALYSIS

A sensitivity analysis was conducted to determine the effect of the variability of the model parameter values on the magnitude of the estimated head loss values. The purpose of the sensitivity analysis was to identify which parameters have the greatest impact on head loss to inform future work with the empirical model. The parameter with the greatest impact can be properly emphasized when designing future honeycomb structures.

The sensitivity analysis was conducted on the empirical model by adjusting the values of each parameter. Each parameter was increased and decreased by 10% and 30% from the mean value in the experimental data. The parameters evaluated were L/D , w/D , y/D and Fr_D as defined by the model. Table 4.1 contains a summary of the sensitivity analysis.

Table 4.9 Summary of Sensitivity Analysis.

Test	Description
1	L/D decreased by 30%
2	L/D decreased by 10%
3	L/D increased by 10%
4	L/D increased by 30%
5	w/D decreased by 30%
6	w/D decreased by 10%
7	w/D increased by 10%
8	w/D increased by 30%
9	y/D decreased by 30%
10	y/D decreased by 10%
11	y/D increased by 10%
12	y/D increased by 30%
13	Fr_D decreased by 30%
14	Fr_D decreased by 10%
15	Fr_D increased by 10%
16	Fr_D increased by 30%

The results of the sensitivity analysis revealed that the model was most sensitive to the variations of the parameter y/D and least sensitive to variation of the parameters w/D and Fr .

Figure 4.10 shows the results of the sensitivity analysis of the empirical model to the parameter L/D . This figure suggests that increasing the length or decreasing the diameter 10% results in an increase in dimensionless head loss of about 5% and that the impact in percent change is about half that of the change in the parameter.

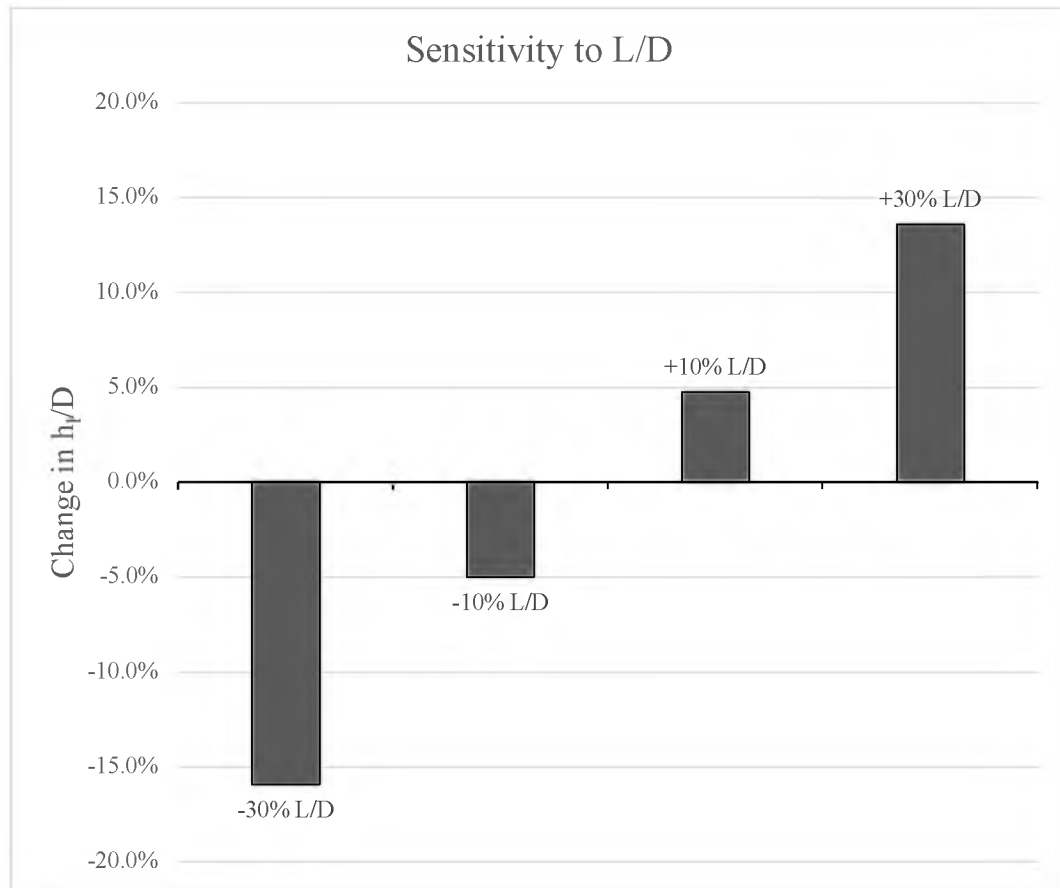


Figure 4.10 The Sensitivity Analysis of the Empirical Model to L/D .

Figure 4.11 shows the results of the sensitivity analysis of the empirical model to the parameter w/D . The figure indicates that increasing the width or decreasing the diameter 10% results in a decrease in dimensionless head loss of about 2%. Also, it suggests the impact in percent change is less than half that of the change in the parameter. The results indicate that the model is not sensitive to the parameter w/D .

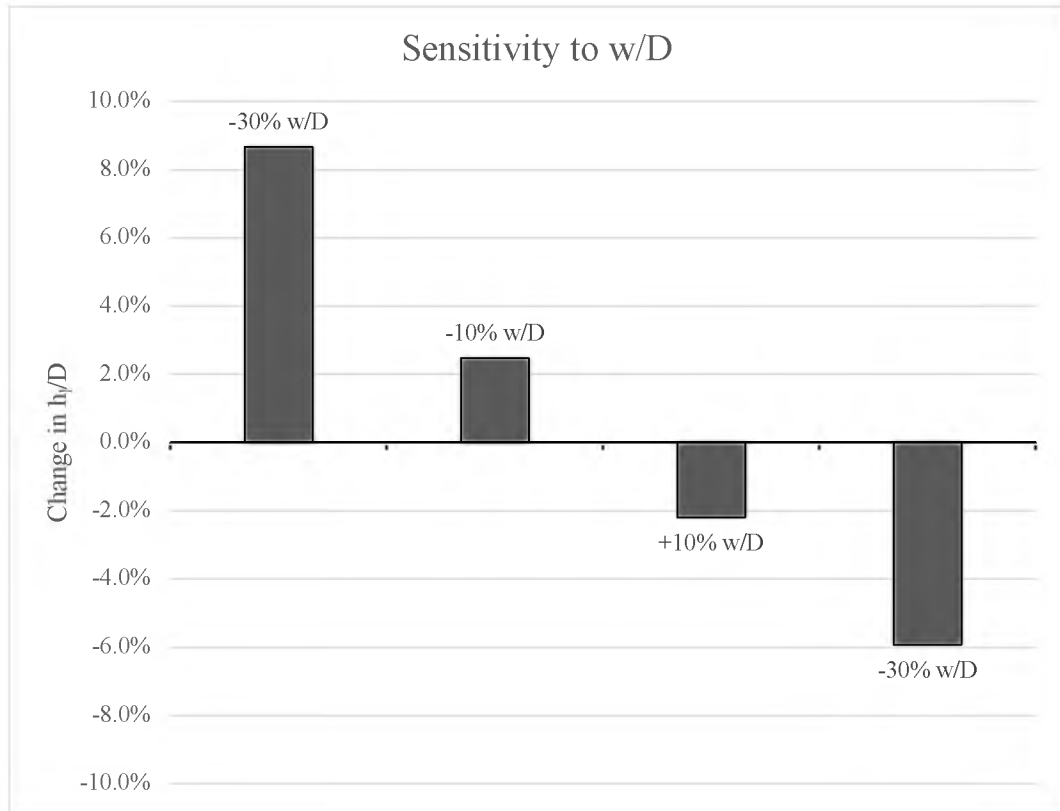


Figure 4.11 The Sensitivity Analysis of the Empirical Model to w/D .

Figure 4.12 shows the results of the sensitivity analysis of the empirical model to the parameter y/D . The figure indicates that increasing the flow depth or decreasing the diameter 10% results in a decrease in dimensionless head loss of about 10% and that the impact in percent change is the same of the change in the parameter. The results indicate that the model is most sensitive to the parameter y/D .

Figure 4.13 shows the results of the sensitivity analysis of the empirical model to the parameter Fr_D . It suggests that increasing the Diameter Froude Number 10% results in a decrease in dimensionless head loss of about 0.5% and that the impact in percent change is negligible to that of the change in the parameter. The results indicate that the model is least sensitive to the parameter Fr_D .

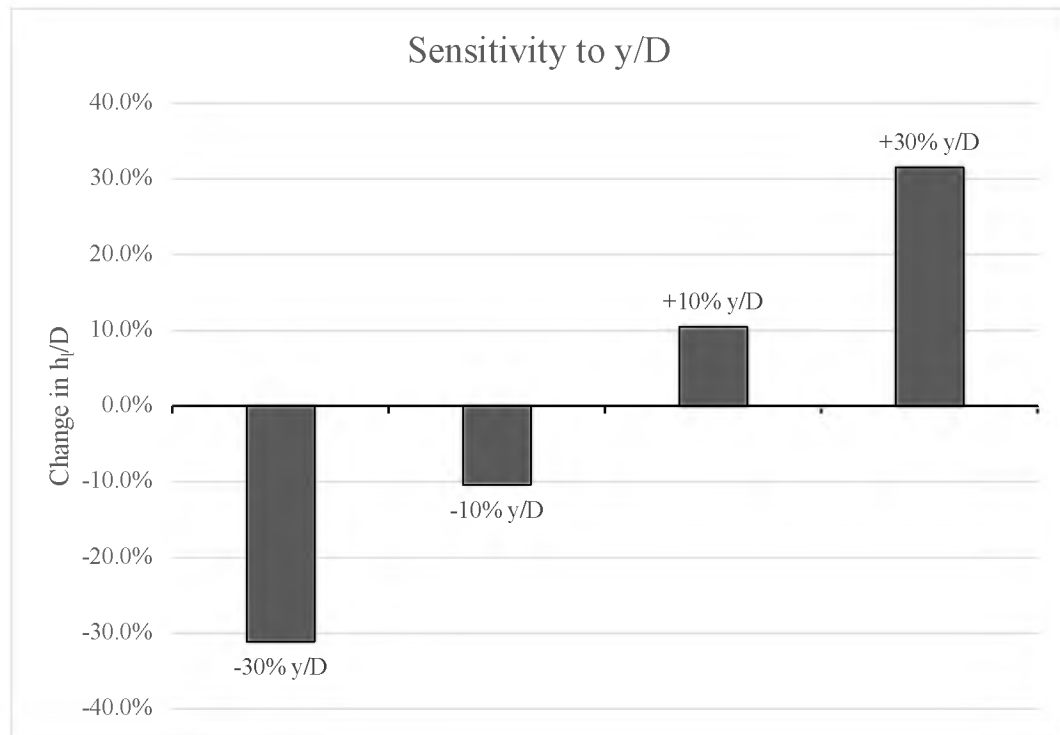


Figure 4.12 The Sensitivity Analysis of the Empirical Model to y/D .

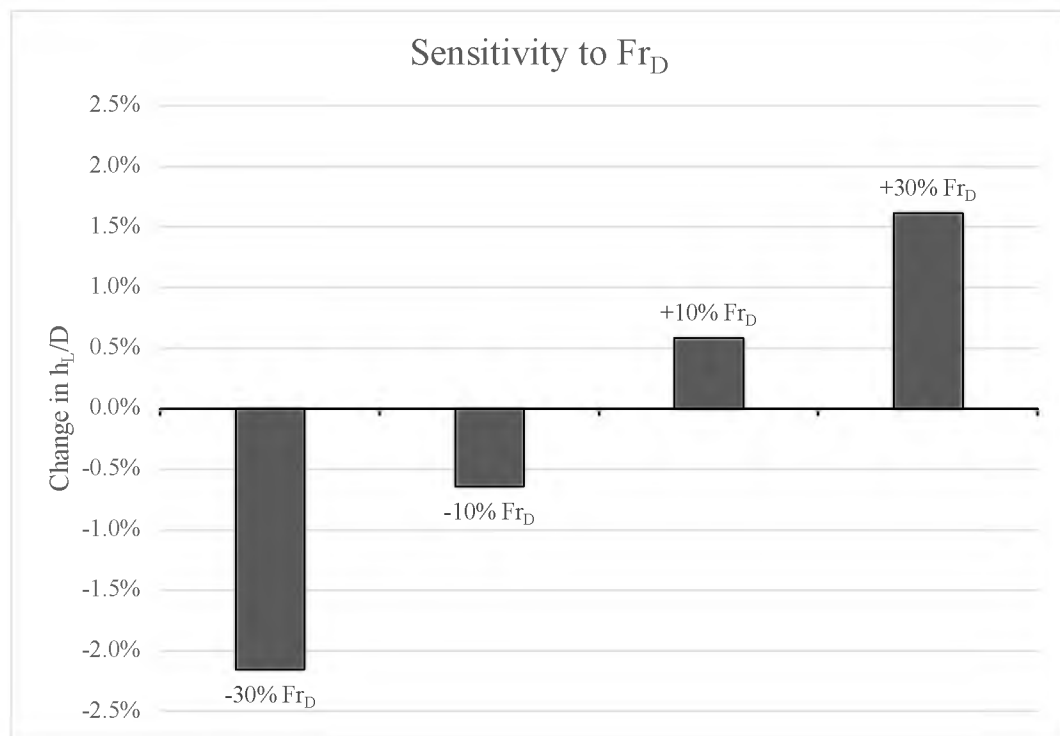


Figure 4.13 The Sensitivity Analysis of the Empirical Model to Fr_D .

In summary, the sensitivity analysis results indicate that the model is most sensitive to the parameter y/D and least sensitive to the parameter Fr_D . The analysis also suggests that changes to pipe length, pipe diameter or depth of flow will have the greatest impact on head loss. Table 4.2 summarizes the results of the sensitivity analysis.

Table 4.10 Sensitivity Analysis Results.

Test	Result
L/D decreased by 30%	Head loss decrease 15.9%
L/D decreased by 10%	Head loss decrease 5.0%
L/D increased by 10%	Head loss increase 4.7%
L/D increased by 30%	Head loss increase 13.6%
w/D decreased by 30%	Head loss increase 8.7%
w/D decreased by 10%	Head loss increase 2.5%
w/D increased by 10%	Head loss decrease 2.2%
w/D increased by 30%	Head loss decrease 5.9%
y/D decreased by 30%	Head loss decrease 31.1%
y/D decreased by 10%	Head loss decrease 10.4%
y/D increased by 10%	Head loss increase 10.5%
y/D increased by 30%	Head loss increase 31.5%
Fr_D decreased by 30%	Head loss decrease 2.2%
Fr_D decreased by 10%	Head loss decrease 0.6%
Fr_D increased by 10%	Head loss increase 0.6%
Fr_D increased by 30%	Head loss increase 1.6%

5. RESULTS AND DISCUSSION

The head loss through a honeycomb structure in open-channel flumes was investigated experimentally. The results of the experimental measurements obtained were processed and used to develop an empirical equation for the energy head loss induced by the honeycomb structure in open channel flows. The empirical model derived was compared to other models.

Additionally, a sensitivity analysis was conducted to determine the most influential parameters. The results of the empirical model development and sensitivity analysis were used to develop a design procedure for honeycomb structures in open channel flows.

In addition to the empirical model derived, three models currently available in the literature were examined and adopted for comparison. The predicted value of h_l/D was plotted against the observed value for each model. The plots also include a line of perfect agreement. Figures 5.1 and 5.2 show the comparison for the Darcy-Weisbach and FHWA models.

Figure 5.1 shows that the Darcy-Weisbach model overpredicts consistently the values of h_l/D . Figure 5.2 indicates that the FHWA model over predicts consistently the values of dimensional head loss h_l/D .

The R-square value for the Darcy model and FHWA model was 0.10 and 0.06, respectively. The results shown in this figure, just as in Figure 5.1, is further supported by the Nash-Sutcliffe coefficient of efficiency in Table 5.1.

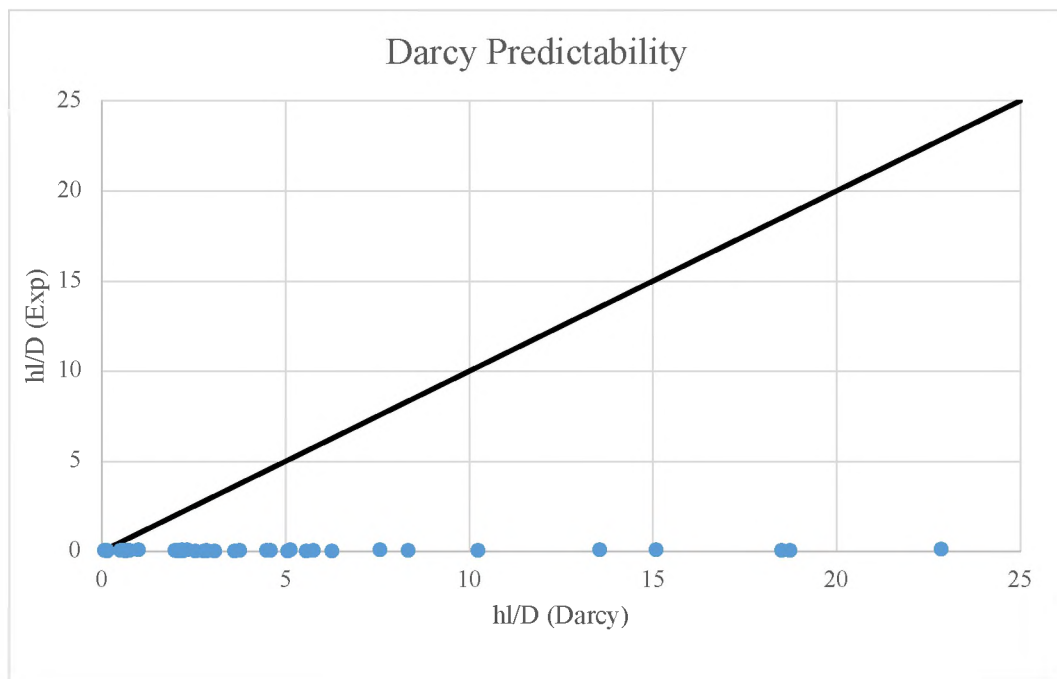


Figure 5.1 The Predictability of the Darcy-Weisbach Model.

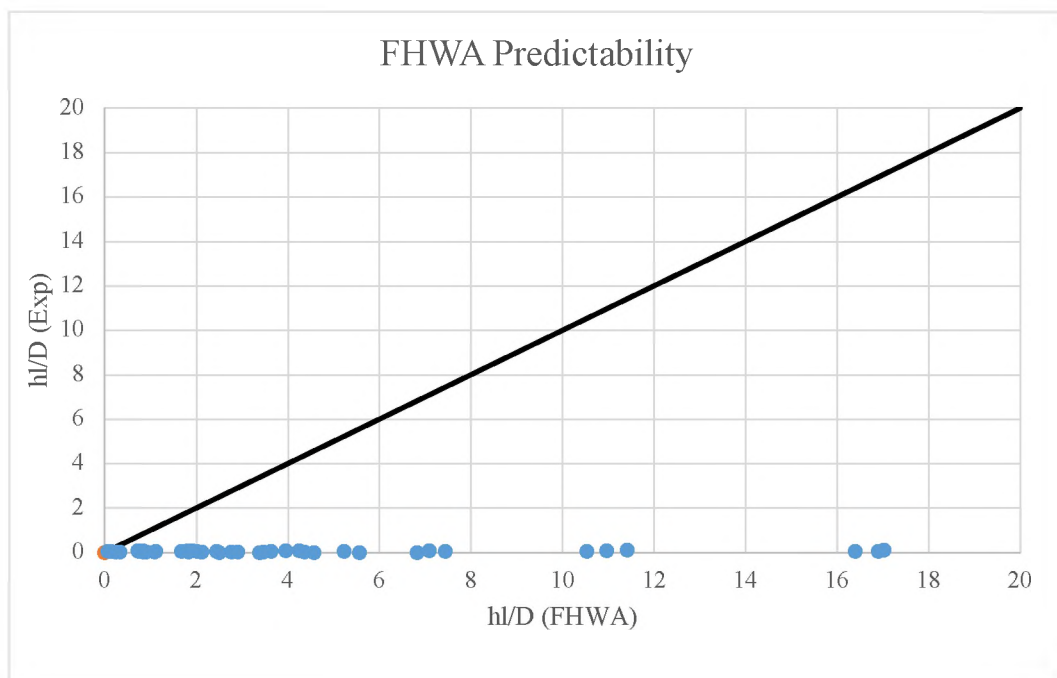


Figure 5.2 The Predictability of the FHWA Model.

Table 5.1 Model Performance.

Model	NSE
Empirical	0.75
Darcy	-72939
FHWA	-53526
Eckert	-16.2

Figure 5.3 shows the plot for the Eckert Model. The plot shows that the model somewhat predicts the values of h_f/D . The plot suggests that the form of the equation is useful, but some adjustments may need to be made. The R-square value for the Eckert model was 0.20. The outlier results in the plot occurred in the test series $D=1/2$. This suggests that the model will under predict the head loss through honeycombs with diameters less than $3/4$ inches.

Figure 5.4 shows the plot for the empirical model. The plot shows that the model predicts the value of h_f/D for the range of parameters tested. The R-square value for the empirical model was 0.76. This figure further supports the usefulness of the empirical model.

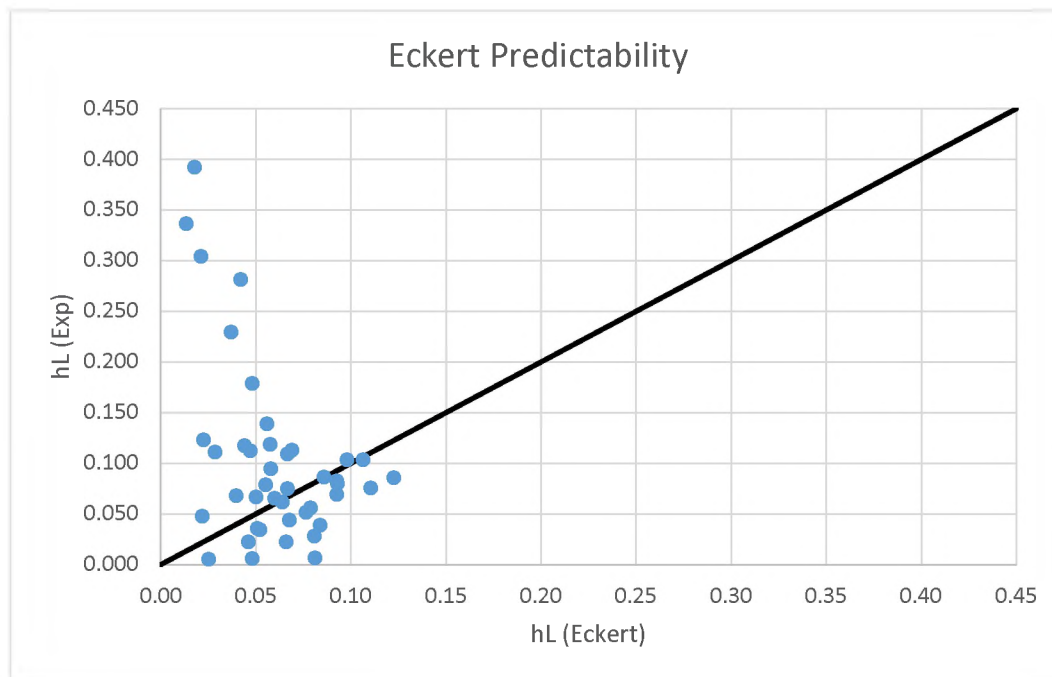


Figure 5.3 The Predictability of the Eckert Model.

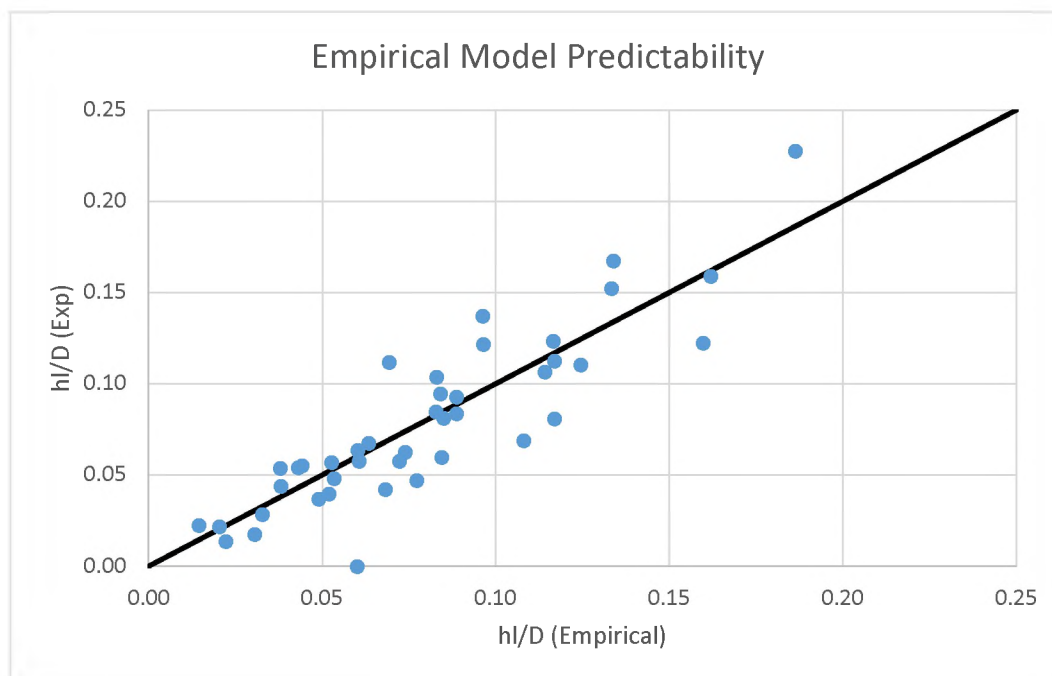


Figure 5.4 The Predictability of the Empirical Model.

The experimental observations of the parameter h_l/D were plotted versus the parameter Diameter Froude Number, $Q/(g^{1/2}D^{5/2})$. The plots were separately prepared for different values of w/D and for different values of the ratio L/D . These plots show that the parameter h_l/D increases with increases of $Q/(g^{1/2}D^{5/2})$ and that greater values of the L/D parameter translate into greater values h_l/D . The plots in Figures 5.1-5.6 depict the observed trend of the value of h_l/D versus the other noted parameters.

The figures show that a greater L/D results in a greater value of h_l/D . Additionally, Figures 5.5-5.10 show that as the discharge increases for a given structure, the head loss also increases. The figures also show that decreasing the diameter of the pipes increases the head loss.

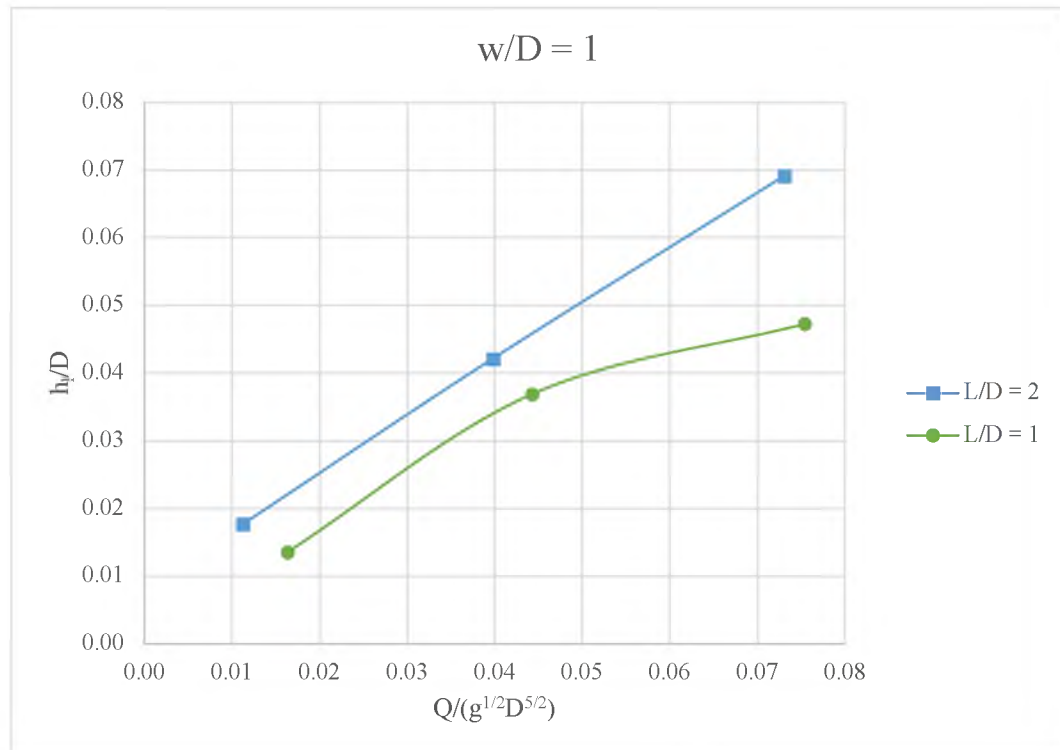


Figure 5.5 The Plot of h_l/D vs $Q/(g^{1/2}D^{5/2})$ for $w/D = 1$.

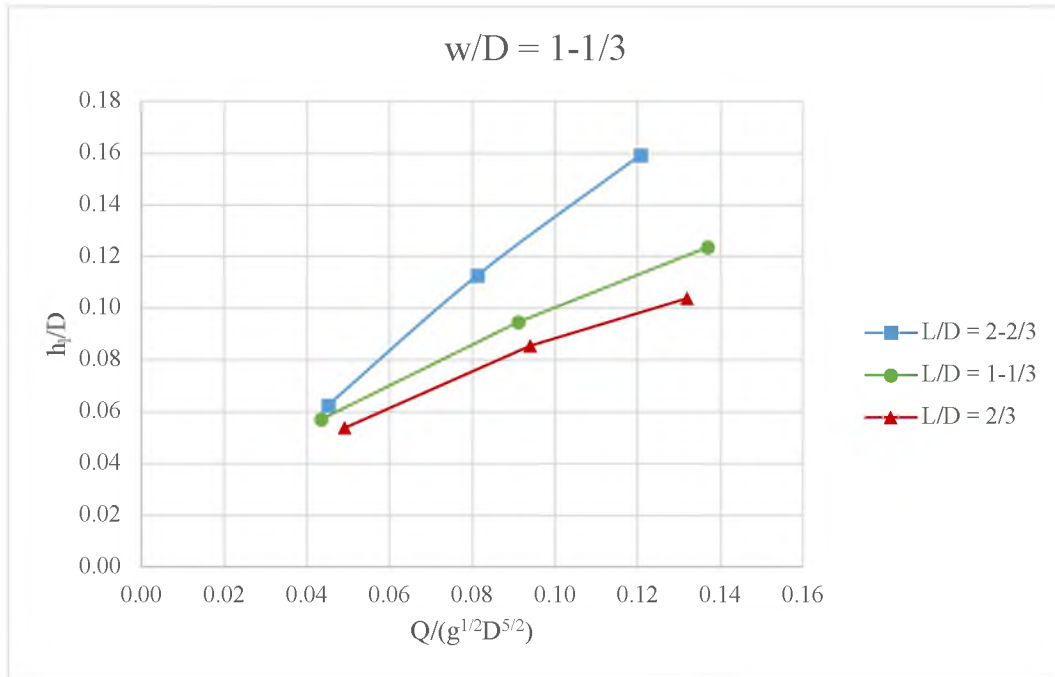


Figure 5.6 The Plot of h_l/D vs $Q/(g^{1/2}D^{5/2})$ for $w/D = 1-1/3$.

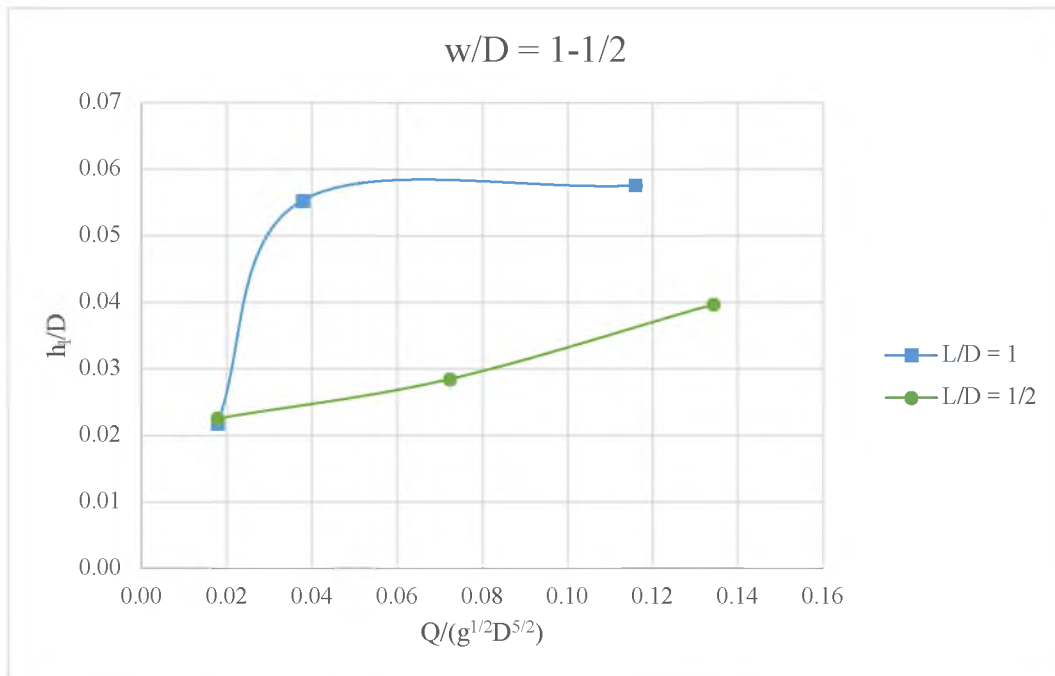


Figure 5.7 The Plot of h_l/D vs $Q/(g^{1/2}D^{5/2})$ for $w/D = 1-1/2$.

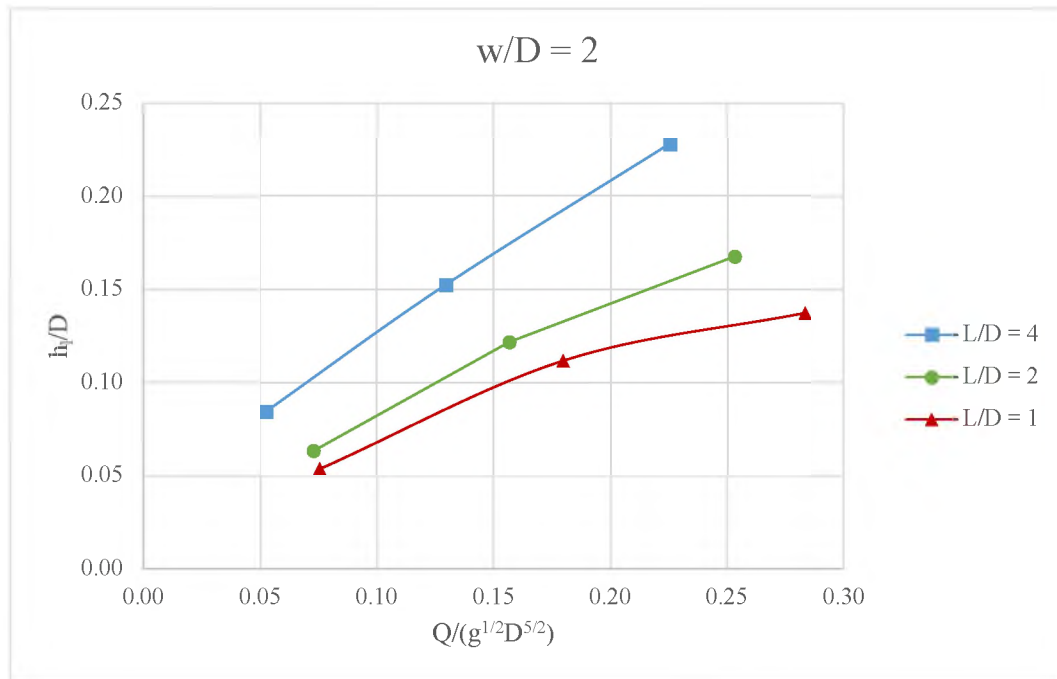


Figure 5.8 The Plot of h_l/D vs $Q/(g^{1/2}D^{5/2})$ for $w/D = 2$.

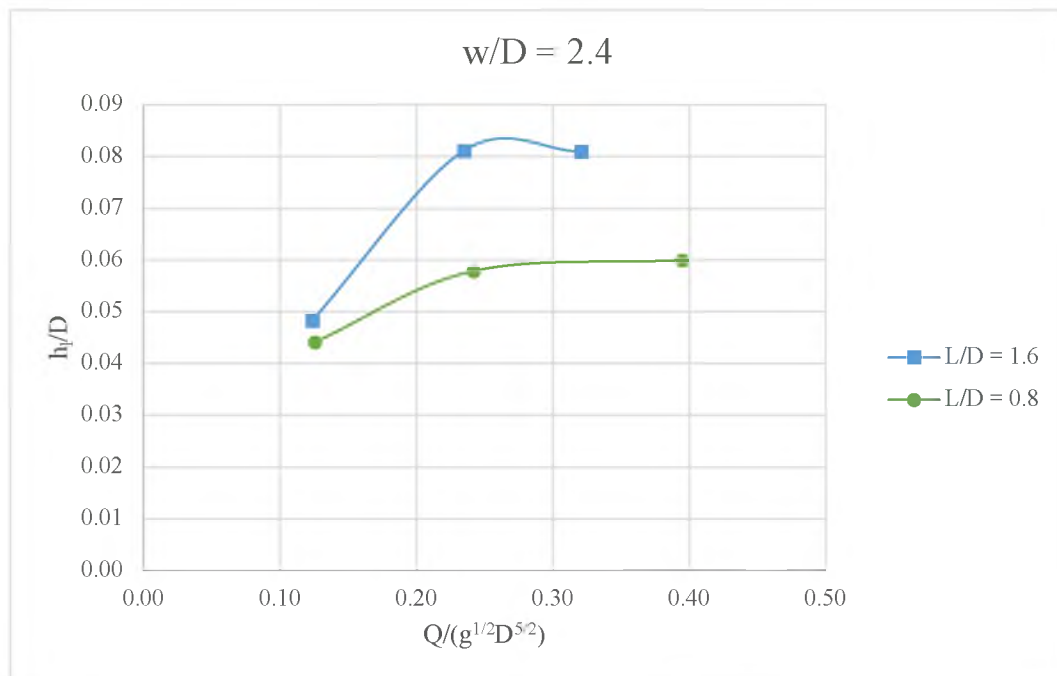


Figure 5.9 The Plot of h_l/D vs $Q/(g^{1/2}D^{5/2})$ for $w/D = 2.4$.

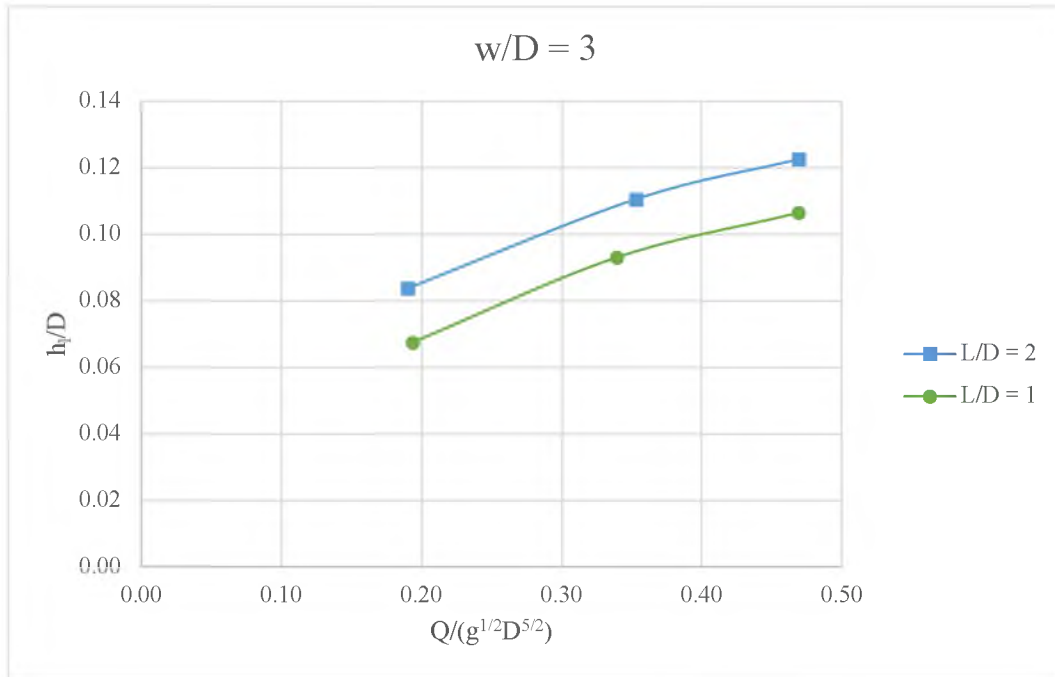


Figure 5.10 The Plot of h_l/D vs $Q/(g^{1/2}D^{5/2})$ for $w/D = 3$.

The empirical model, Equation 31, and the figures above, Figure 5.5 to 5.10, serve as design tools for honeycomb structures in open channel flows. For the range of parameters tested, the empirical model can be solved directly for a given unknown if the other parameters are provided. In situations with multiple unknown parameters, Figures 5.5-5.10 provide design charts. Given a discharge and channel geometry, the pipe diameter is selected, and the parameter w/D is determined. The corresponding w/D chart will then provide information to select the pipe length for the honeycomb structure. The model equation and the charts will also allow the discharge to be determined if the geometry of the channel and the honeycomb structure are known as well as the head loss through the structure.

6. CONCLUSIONS AND RECOMMENDATIONS

The results of this work provide a means to predict the head loss through a honeycomb structure in an open channel. Additionally, a procedure for designing structures was also outlined. Multiple approaches were considered, and the empirical model was found to be best suited to predict the energy head loss across the honeycomb structure.

This work found that the application of currently available models was insufficient to predict accurately head loss. Both the applied Darcy-Weisbach and the FHWA models over-predicted the head loss for the structure. The Eckert model showed some potential for application; however, some adjustments will be required for improvement. All the considered existing models produce negative NSE values, which indicate poor prediction ability. The empirical model developed from the statistical analysis of the collected data best predicted the head loss. The model had NSE values of 0.83 and 0.75 for the development and validation data respectively.

The empirical model was most sensitive to the y/D parameter. The value of h_l/D increased and decreased by the same percentage as y/D . Increasing and decreasing the value of L/D caused an increase and decrease of h_l/D by half the percentage of change in L/D . The value of h_l/D decreased and increased one fifth the percentage of increase and decrease in w/D . The Fr_D parameter was shown to change the value of h_l/D one fifteenth of the percentage of the change of Fr_D . The most influential parameter was shown to be y/D while the least influential parameter was shown to be Fr_D .

The experimental work showed general trends in the head loss for given parameters. For a given w/D , increasing L/D resulted in increased h_f/D . For a given w/D and L/D , increasing the discharge resulted in an increase in h_f/D . The results also showed that decreasing the diameter lead to an increase in the head loss. The results provide general design guidance for honeycomb structures.

The result of this work provided an empirical model and charts for design. The empirical model directly calculates the head loss when the discharge, width, flow depth, pipe length and pipe diameter are known. Figures 5.5-5.10 are design charts and narrow down possible dimensions for a given application. The work resulted in a design procedure for honeycomb structures. First, the design discharge and channel geometry are collected. The width of the channel is in feet and the design discharge is in cubic feet per second. Then a pipe diameter is selected, in inches, and the corresponding design chart is considered. The design chart is then used to select a length of pipe, in feet, to meet the design requirements. Finally, the head loss, in feet, for a given discharge through the selected structure geometry can be predicted using the model. It should be noted that the empirical model was determined from the range of parameters examined. The empirical model is valid for a range of discharges from 0.053 to 4.310 cubic feet per second, a range of pipe diameters from $\frac{1}{2}$ to 2 inches, a range of pipe lengths from 0.5 to 2 feet, a range of y/D from 1 to 5, and a range of channel widths from 1 to 3 feet. The greatest impact on the predicted head loss is the parameter, y/D . y/D represents the flow depth, in inches, to pipe diameter in inches.

This work evaluated honeycomb structures in a wide range of discharges and geometries and provided design guidance for applications within these ranges. The

performance of honeycombs of different materials, orientations, and in larger discharges has yet to be investigated. Additionally, the impact of honeycomb structures on the erosion of a bed of erodible material, the impact of the combination of honeycombs and screens, and the calibration of the Eckert's model equation for honeycombs in open channel flows have yet to be investigated.

BIBLIOGRAPHY

1. Prandtl, L., *Attaining a steady air stream in wind tunnels*. 1933.
2. Barlow, J.B., W.H. Rae, and A. Pope, *Low-Speed Wind Tunnel Testing*. Third ed. 1999: John Wiley & Sons.
3. Scheiman, J. and J. Brooks, *Comparison of experimental and theoretical turbulence reduction from screens, honeycomb, and honeycomb-screen combinations*. Journal of Aircraft, 1981. **18**(8): p. 638-643.
4. Idelcik, I., *Handbook of hydraulic resistance: coefficients of local resistance and of friction*. 1966, ERDA Div. Phys. Res.
5. Lumley, J., *Passage of a turbulent stream through honeycomb of large length-to-diameter ratio*. 1964.
6. Lumley, J.L. and J. McMahon, *Reducing water tunnel turbulence by means of a honeycomb*. 1967.
7. Jiang, Y., et al. *The hydrodynamic design and critical techniques for 1m× 1m water tunnel*. in *AIP Conference Proceedings*. 2018. AIP Publishing LLC.
8. Yeh, H.H. and M. Shrestha, *Free-surface flow through screen*. Journal of Hydraulic Engineering, 1989. **115**(10): p. 1371-1385.
9. Çakir, P., *Experimental investigation of energy dissipation through screens*. 2003, Citeseer.
10. Tsikata, J.M., *Experimental investigation of turbulent flow through trashracks*. 2008.
11. White, F.M., *Fluid Mechanics*. Fourth ed. 2010: McGraw-Hill.
12. Transportation, T.D.o., *Hydraulic Design Manual*. 2019, TxDOT Austin, Tex.: Austin, Texas, United States of America.
13. Mays, L.W., *Water resources engineering*. Second ed. 2010: John Wiley & Sons.
14. Mohammed-Ali, W., *Hydraulic characteristics of semi-elliptical sharp crested weirs*. J. Int. J. v. Giraldez Rev. Civil Eng, 2012. **1**: p. 13.
15. Nash, J.E. and J.V. Sutcliffe, *River flow forecasting through conceptual models part I—A discussion of principles*. Journal of hydrology, 1970. **10**(3): p. 282-290.

16. Mohammed-Ali, W., C. Mendoza, and R.R. Holmes Jr, *Influence of hydropower outflow characteristics on riverbank stability: case of the Lower Osage River (Missouri, USA)*. Hydrological Sciences Journal, 2020.
17. Mohammed-Ali, W., C. Mendoza, and R.R. Holmes, *Riverbank stability assessment during hydro-peak flow events: The lower Osage River case (Missouri, USA)*. International Journal of River Basin Management, 2020: p. 1-9.

VITA

Kyle David Hix received his B.S. in Civil Engineering in December 2018 from Missouri University of Science and Technology. He also received his M.S. in Civil Engineering from Missouri University of Science and Technology in August 2020.